

Energy dissipation in the dynamics of a bouncing ball

K. Szymanski^{1,2,*} and Y. Labaye^{1,†}

¹Laboratoire de Physique de l'Etat Condensé, UPRESA CNRS 6087, Université du Maine, 72085 Le Mans, Cedex 09, France

²Institute of Physics, University at Białystok, Lipowa 41, 15-424 Białystok, Poland

(Received 15 July 1998)

A horizontally bouncing ball between a rigid wall and a sinusoidally vibrating plate is investigated analytically, numerically, and experimentally. Transient chaotic and chattering modes show substantially different shock power dissipation from that of resonant movement. Gain of the dissipated shock power is observed when the system enters into periodic modes. Period doubling routes to chaos have no substantial influence on the shock power. Connections of the proposed model with dynamics of mechanical alloying processes are discussed. [S1063-651X(99)07403-6]

PACS number(s): 05.45.-a, 45.05.+x, 46.80.+j, 46.90.+s

I. INTRODUCTION

Physics related to the dynamics of a bouncing ball has started to be relevant since Fermi proposed that cosmic radiation originates from charged particles accelerated by moving magnetic field structures [1]. Then Ulam examined the problem of a ball moving between a rigid wall and a vibrating plate without dissipation [2]. The dynamics of the bouncing ball was considered as an example showing stochastic behavior resulting from nonrandom forces [3]. The physics of ergodicity, i.e., filling of the available phase space by stochastic motion, was also discussed for different mappings originating from the bouncing ball model [4]. In other respects, Mehta and Luck reported on the influence of a gravitational field on a completely inelastic bouncing ball on a vertically vibrating plate [5]. The same authors then discussed the dynamics of a bouncing ball with a finite coefficient of restitution: exact mapping estimates, transient chaotic motion, chattering, and locking [6]. The last phenomena are processes in which a ball performs an infinite number of impacts in a finite time with complete loss of both energy and memory of initial conditions. Phase portraits of the system had previously been measured experimentally by Kowalik *et al.* [7]. Recently, Drossel and Prellberg described the dynamics aspects of a single particle in a horizontally shaken box [8]. Less theoretical problems connected to the applications were presented by Valance and Bideau [[9] and references therein] where the movement of the ball on a rough surface was considered.

During the last decade, great attention was devoted to mechanical alloying or high-energy ball milling—technological processes for making ultrafine amorphous or nanostructured powders. The mechanisms involved in such processes are closely related to the dynamics of the bouncing ball. Indeed, during mechanical alloying, the solid-state reaction is driven by the energy released during the collisions between macroscopic objects (usually balls inside a vial) in the presence of a reacted medium (usually micrometer size powders). Important parameters of the kinetics of ball mill-

ing are shock power, impact time, and energy of a single impact and were determined by studies of different models approaching real devices [10–12]. We think that the dynamics of mechanical alloying can be supported by a model for which solutions can be obtained without simplified assumptions.

We characterize the behavior of the model which depends on only two dimensionless parameters: relative size of the system and restitution coefficient. Our one-dimensional model consists of a rigid wall, a vibrating plate, and an object moving horizontally between the wall and plate. The choice of such a model was motivated by the possible construction of an experimental device which allows us observation and measurements of the dynamic quantities. The dynamics of the model is explored both analytically and/or numerically. We will show that collisions (or modes) are of basically three types: (1) high-energy periodic modes which exhibit period doubling routes to chaotic solutions with nearly unchanged energy characteristics, (2) short-period chattering and locking in which small amount of energy is dissipated, and (3) chaotic or long-periodic modes. The first type of collisions will be called resonant, the others nonresonant. The energy dissipation for nonresonant modes is given by simple expression. A remarkable gain of shock power is observed in the simulations as well as in the experimental approach when the system enters into resonant mode.

II. MODEL

Let us consider a one-dimensional system in which a small ball is moving freely between a rigid wall and a vibrating plate. The position of the plate is given by $x(t) = A \sin(\omega t)$, where A and ω represent the amplitude and frequency, respectively. The plate is separated from the wall by an average distance L , $L > A$. The ball collides elastically with the wall while collisions with the plate (shocks) are partially elastic, characterized by restitution coefficient k . In the system of plate $k = |v'_a/v'_b|$, where v'_b and v'_a are velocities before and after the shock, respectively.

For convenience, let us transform our prime variables to dimensionless ones: $v_i = v'_i/A\omega$, $t_i = \omega t'_i$. Our system is characterized by two dimensionless parameters: the restitution coefficient of k and the relative size of the system, α

*Electronic address: kszym@alpha.uwb.edu.pl

†Electronic address: yvan@univ-lemans.fr

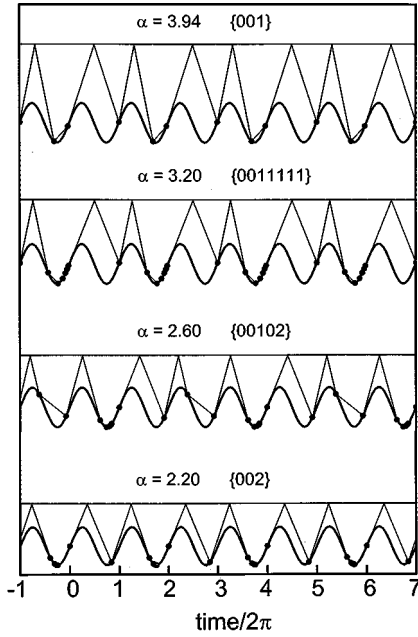


FIG. 1. Sequence of periodic modes for $k=0.46$ and indicated values of α . The $\{j_i\}$ series is shown for every mode. The Y axis represents the increasing distance between the plate and wall (i.e., increasing value of α).

$=L/A$. In the dimensionless notation, the amplitude of plate vibration is equal to 1 and the vibration period to 2π . We use the notation in which v_i is the velocity of the ball after shock at time t_i , before interaction with the wall or the plate.

After interaction with the wall, the ball interacts with the plate. The next interaction can be with either the wall or plate. For a description of a series of shocks, we introduce the following notation. Integer 0 describes the shock and next interaction with the wall. Integer 1 describes the shock and next interaction with the plate. Thus a series of shocks can be represented by a series of integers $\{j_i\}$. For the periodic mode it is enough to write integers corresponding to one period of the $\{j_i\}$; so the simplest periodic mode has the abbreviation $\{0\}$. The sequence of infinite numbers of shocks with the plate corresponding to chattering will be abbreviated by integer 2. The simplest chattering mode is thus $\{0,2\}$. Figure 1 illustrates several modes of the periodic movement and its $\{j_i\}$ abbreviations. Examples of chattering are observed for $\alpha=2.6$ and 2.2 . We will use $\{j_i\}$ in the construction of the map, and so we need a more formal definition of j_i for further consideration. Let us define a positive, continuous, and periodic function $v^+(t)$ with period 2π : $v^+(t) = \cos(t)$ for $2\pi m \leq t \leq 2\pi m + \pi/2$, $m=0, \pm 1, \pm 2, \dots$, and for other t values, $v^+(t)$ is equal to the positive slope of the straight line which crosses point t on the sinusoid and which is tangent to the sinusoid at point t_0 , $t < t_0 < t + 2\pi$. The function $v^+(t)$ has a clear physical interpretation: $v^+(t_i)$ represents a critical value of velocity for the ball after shock at time t_i . If $v_i \geq v^+(t_i)$, the ball interacts with the wall and then with the plate; if $v_i < v^+(t_i)$, the ball interacts only with the plate. Now series $\{j_i\}$ can be defined formally: $j_i = 1 - \theta_+(v_i - v^+(t_i))$, where θ_+ is the Heaviside functions: $\theta_+(x) = 0$ for $x < 0$, $\theta_+(x) = 1$ for $x \geq 0$.

Let us define the mapping $F: t_i, v_i \rightarrow t_{i+1}(t_i, v_i)$,

$v_{i+1}(t_i, v_i)$. The difficulty arises because one cannot write the map explicitly. The time of the next shock, t_{i+1} , is given by the smallest root of the nonlinear equation, for which $t_{i+1} > t_i$. The equation has a form depending on j_i :

$$2\alpha - \sin t_i - \sin t_{i+1} = (t_{i+1} - t_i)v_i \quad \text{for } j_i = 0, \quad (1a)$$

$$\sin t_{i+1} - \sin t_i = (t_{i+1} - t_i)v_i \quad \text{for } j_i = 1. \quad (1b)$$

Equation (1a) states that the path traveled by the ball between shock at time t_i , interaction with the wall, and next shock at time t_{i+1} is equal to the ball velocity multiplied by the time between shocks. Equation (1b) describes two consecutive shocks (i.e., no interaction with the wall for time comprised between t_i and t_{i+1}). The velocity v_{i+1} follows from usual definition of the restitution coefficient k and is expressed by

$$v_{i+1} = kv_i + (1+k)\cos t_{i+1} \quad \text{for } j_i = 0, \quad (1c)$$

$$v_{i+1} = -kv_i + (1+k)\cos t_{i+1} \quad \text{for } j_i = 1. \quad (1d)$$

The dimensionless energy dissipated during shock at time t_i is equal to

$$\varepsilon_i = (1-k^2)(\cos t_i + v_{i-1})^2 \quad \text{for } j_i = 0, \quad (2a)$$

$$\varepsilon_i = (1-k^2)(\cos t_i - v_{i-1})^2 \quad \text{for } j_i = 1 \quad (2b)$$

where $\varepsilon_i = 2E_i/\mu A^2 \omega^2$, E_i corresponds to the energy dissipated during the shock, and μ corresponds to the mass of the ball. In the same way we can define the dimensionless shock power dissipated during shock series $\{j_i\}$, $i = 1, \dots, N$:

$$p = \frac{\sum_{i=1}^N \varepsilon_i}{t_N - t_1}, \quad (2c)$$

where $p = 2P/\mu A^2 \omega^3$ and P is the shock power.

III. SIMPLE PERIODIC SOLUTIONS

We first consider the movement with $j_i = 0$ for all i . Without loss of generality, we can introduce the variable $\tau_i = t_i - 2\pi Mi$, where M is a positive integer. It follows Eqs. (1a) and (1c) that the mapping of this movement, $F, \tau_i, v_i \rightarrow \tau_{i+1}(\tau_i, v_i), v_{i+1}(\tau_i, v_i)$, is given implicitly by a pair of equations

$$v_{i+1} = kv_i + (1+k)\cos \tau_{i+1}, \quad (3a)$$

$$2\alpha - \sin \tau_i - \sin \tau_{i+1} = (2\pi M + \tau_{i+1} - \tau_i)v_i. \quad (3b)$$

The movement with periodicity $2\pi M$, which will be abbreviated as L_M , corresponds to the fixed point τ^*, v^* of the mapping (3):

$$\sin \tau^* = \frac{\alpha(\kappa/\pi M)^2 \pm \sqrt{1 - (\kappa/\pi M)^2(\alpha^2 - 1)}}{1 + (\kappa/\pi M)^2}, \quad (4a)$$

$$\cos \tau^* = \frac{\kappa}{\pi M} \frac{\alpha \mp \sqrt{1 - (\kappa/\pi M)^2(\alpha^2 - 1)}}{1 + (\kappa/\pi M)^2}, \quad (4b)$$

$$v^* = \frac{\cos \tau^*}{\kappa}, \quad (4c)$$

where $\kappa = (1-k)/(1+k)$.

Solutions (4) with upper signs are unstable. To find the stability of L_M , we apply the procedure given in [13] and expand the operator F in the vicinity of the fixed point τ^*, v^* of Eqs. (4). Perturbing a fixed point by $\delta\tau_i$ and δv_i , respectively, one can find F' , the first derivative of F :

$$\begin{aligned} \begin{pmatrix} \delta\tau_{i+1} \\ \delta v_{i+1} \end{pmatrix} &= F' \begin{pmatrix} \delta\tau_i \\ \delta v_i \end{pmatrix} \\ &= \begin{pmatrix} k & -(1-k) \frac{\pi M}{\cos \tau^*} \\ -k(1+k) \sin \tau^* & k + \pi M(1-k^2) \tan \tau^* \end{pmatrix} \\ &\quad \times \begin{pmatrix} \delta\tau_i \\ \delta v_i \end{pmatrix}. \end{aligned} \quad (5)$$

If the modulus of one of the eigenvalues of F' is smaller than 1, the fixed point is stable. This condition can be written for two-dimensional maps in terms of invariants: determinant $\text{Det } F'$ and trace $\text{Tr } F'$. If $\text{Tr } F' - \text{Det } F' = 1$, one of the eigenvalues crosses the unit circle at point +1 of the complex plane and saddle node bifurcation occurs. If $\text{Tr } F' + \text{Det } F' = 1$, one of the eigenvalues crosses the unit circle at point -1, giving rise to period-doubling bifurcation. Saddle node bifurcation takes place at the point where the square root in Eqs. (4a) and (4b) is zero, at $\alpha(k) = \alpha_1$, where

$$\alpha_1 = \sqrt{1 + \left(\frac{\pi M}{\kappa}\right)^2}, \quad (6a)$$

while the condition for the period-doubling border is expressed as $\alpha(k) = \alpha_2$, where

$$\alpha_2 = \frac{\pi^2 M^2 - 1}{\sqrt{(\pi M \kappa)^2 + 1}}. \quad (6b)$$

The stability of movement in the region given by Eqs. (6a) and (6b) is governed by the local properties of Eqs. (4). However, the movement corresponding to Eq. (6b) for k close to 0 cannot be realized because the ball trajectory would cross that of the plane. To find the border $\alpha(k)$, for which the mode L_M does not exist, we write

$$v^* = v^+(\tau^*), \quad (7)$$

and substitute t^* and v^* from Eqs. (4)–(7). Expanding Eq. (7) in the vicinity of $\alpha = \pi M$ and $k=0$ up to the first two terms, we get an explicit form $\alpha(k) = \alpha_3$, where

$$\alpha_3 = \pi M - \frac{4}{3} \sqrt{3k} + O^2(\sqrt{k}). \quad (8)$$

For α smaller than α_3 , the L_M mode is replaced by a mode with periodicity $2\pi M$ and with shock sequence $\{j_i\} = \{01\}$. Summarizing, the L_M mode is stable in the region of the α - k plane where $\alpha(k) < \alpha_1$, $\alpha(k) > \alpha_2$, and $\alpha(k) > \alpha_3$.

The shock power of the L_M mode can be derived from Eqs. (2) and (4):

$$p = \frac{2 \cos^2 \tau^*}{\pi M \kappa}. \quad (9)$$

For a given κ , the shock power attains its maximum value if $\cos \tau^* = 1$. It follows from Eq. (4b) that maximum power is dissipated for $\alpha(k) = \pi M / \kappa$.

IV. INFLUENCE OF EXTERNAL NOISE

Let us consider a Poincaré section [13] of the phase space of the low period and stable mode. The section consists of a few points for the mode without chattering and an infinite number of points tending to a point where the velocity of the ball begins to stick on the plate in the case of a chattering mode. The area in the close neighborhood of each point belongs to the domain of attraction of the mode [14]. Let us expose control parameter of the system to external noise. If the noise is small, the section is located within the domain of attraction of the mode and consists of spots centered at undisturbed points. In the case of high noise, the domain of attraction of another mode can be visited. This second domain of attraction behaves like the first one: it may trap the trajectory, or the system may visit other domains of attraction. The detailed evolution will be considered in the following examples.

For $k=0.593$ and $\alpha=2.482$, there exist three stable modes: the chattering mode of $\{000010000000102\}$ type, with period 18π , $\{01\}$ resonance with period 2π , and $\{00\}$ resonance with period 2π . In Fig. 2(a) the phase and velocity at reflection of the chattering mode are shown when exposed to the external noise of restitution coefficient k . The noise is introduced by adding to the mean value of k a number IR after each iteration, where I is the amplitude of the noise and R are the random numbers having the normal distribution. The noise with amplitude 1×10^{-7} causes the formation of a spot in the vicinity of each point. The 3 times larger noise [Fig. 2(b)] causes a temporary visit of the large area of the phase space and the system enters into the domain of attraction of one of the resonances. Starting from the initial conditions corresponding to the $\{01\}$ mode and applying the noise of the amplitude 2×10^{-3} , after 5000 iterations we observe only two spots [Fig. 2(c)], while noise 3×10^{-3} causes visiting a large region of the phase space [Fig. 2(d)]. The movement consists of chaotic and regular series which cause a concentration of the points in the vicinity of the stable points of the $\{01\}$ and chattering modes seen in Fig. 2(d). Starting from the initial conditions of $\{00\}$ resonance, we observe the effect of spot formation for noise with amplitude 3×10^{-3} [Fig. 2(e)] and explosion to the large volume of the phase space for an amplitude of 4×10^{-3} [Fig. 2(f)].

The examples presented suggest a method for choosing initial conditions which correspond to the most stable mode: (i) take any initial conditions, (ii) start iterations with a large noise, and (iii) then decrease the level of noise. The noise has the form $\delta_i = IR \exp(-ib)$, where b is decay constant. The restitution coefficient k is modified by a noise leading to $k_i = k + \delta_i$. Applying a strong enough initial noise

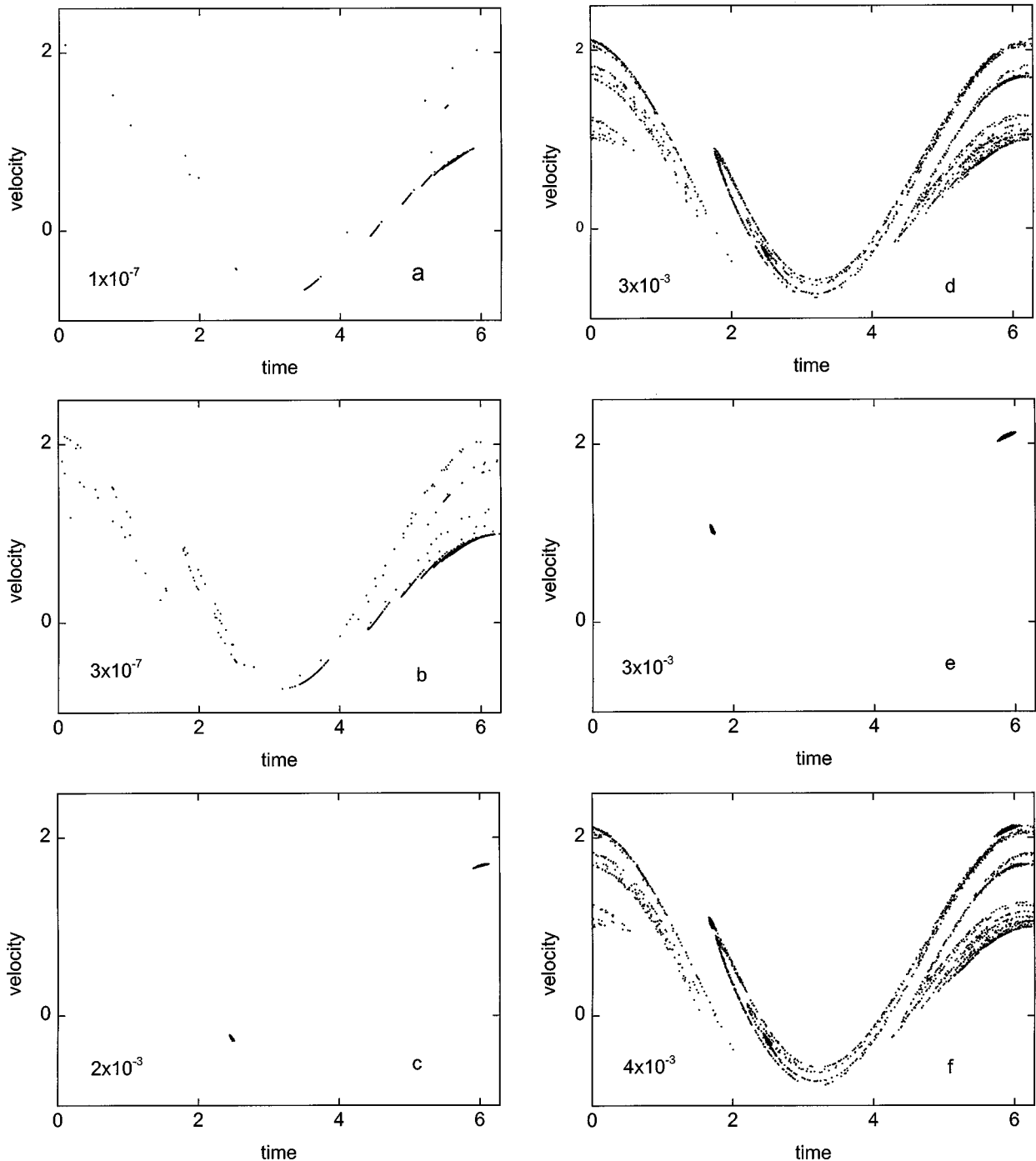


FIG. 2. Velocity and phase of the shocks starting from initial conditions $t=0.0$, $v=0.0$ (a), (b), $t=2.47$, $v=0.54$ (c), (d), and $t=1.69$, $v=1.16$ (e), (f). The α and k parameters were equal to 2.482 and 0.593, respectively. Points corresponding to 5000 iterations are shown under applied Gaussian noise to the k parameter. The amplitude of the noise is shown in each figure.

and reasonable b , we have found that, for a large part of α - k plane, the final state does not depend on the initial condition (e.g., initial velocity and phase). By means of such a method based on the ‘‘noise-decreasing initial condition’’ (NDIC), we performed a scan of some parts of the α - k plane, which is summarized in the next section.

V. CHARACTERIZATION OF THE α - k PLANE

A. Region for α/π of the order of magnitude of 1

The region of the α - k plane for α approximately equal to a few π remains very complex. An illustration is given in

Fig. 3(a), which displays a scan for arbitrarily chosen $k=0.55$. Below the points indicating shock power, we draw a step function, the higher value of which shows the presence of chattering modes, while a lower value indicates that chattering does not occur during the iterations. In Fig. 3(b), short periods of the movement are shown in a similar way. Characteristic features, a few listed below, can be observed.

(i) Silent modes. Sharp minima of the shock power occur at $\alpha=(n+1/2)\pi$, $n=1,2,3,\dots$. Detailed analysis shows that these modes correspond to the simplest chattering modes of $\{02\}$ type with period $T=2\pi n$. It is reasonable to call these modes as silent because, in the experimental observations

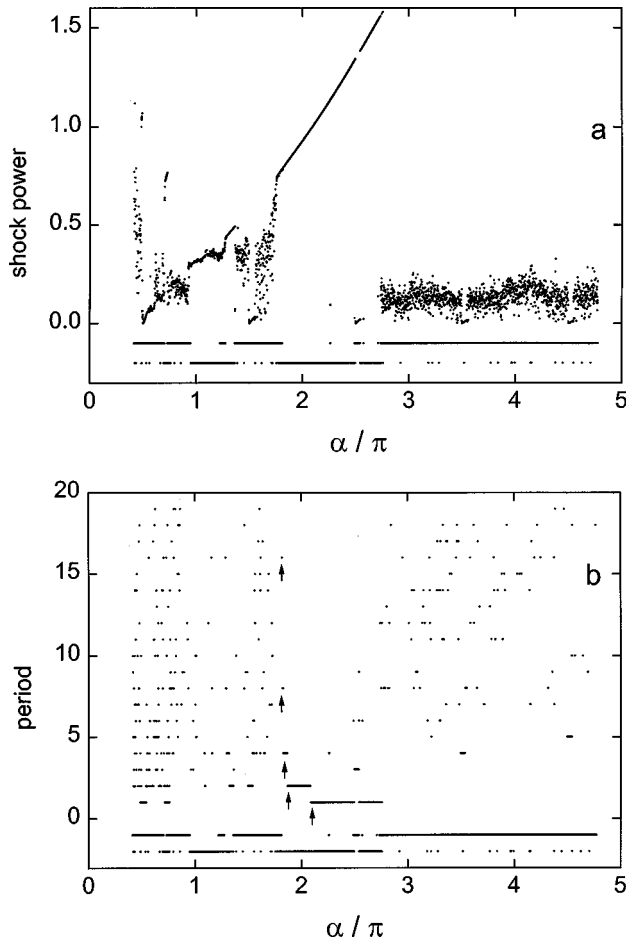


FIG. 3. Shock power (a) and period (b) versus the α parameter for $k=0.55$. Below the points, the step function shows the presence of the chattering mode (higher value) or the lack of chattering (lower value). The points corresponding to a period larger than 10 are not shown in (b). The arrows indicate the period-doubling route to chaos for the L_1 mode. The starting conditions were prepared by the NDIC: $I=0.01$, $b=0.01$, and 3000 iterations were performed.

(see Fig. 7), they produce a very weak sound; in our model dissipater shock power for $\alpha=(n+1/2)\pi$, $n=1,2,3,\dots$, is zero, whatever the k value is.

(ii) Gain of the shock power. In the regions of α where the step function changes its value, a gain of the shock power is observed: the shock power of modes without chattering is larger than those with chattering.

(iii) Noise resistance of the resonances. When the α value decreases below $\alpha_2=2.09\pi$, one observes a period-doubling route to chaos for the L_1 mode [see arrows in Fig. 3(b)]; when α increases, the L_1 mode becomes sensitive to external noise and is replaced by the chattering one, quite far from the stability border, $\alpha_1=3.46\pi$. All resonances observed show a similar behavior. It seems to be a rule that resonances are most resistant against external noise in the region close to its period-doubling border.

(iv) Shock power of the resonances. When α decreases, a series of period-doubling bifurcations of the resonance does not change the character of the shock power [see Fig. 3(a)] in the vicinity of $\alpha\approx 2\pi$. For all resonances observed in computer simulations, in the region of their large noise resistance, the shock power increases with α . This is in agreement

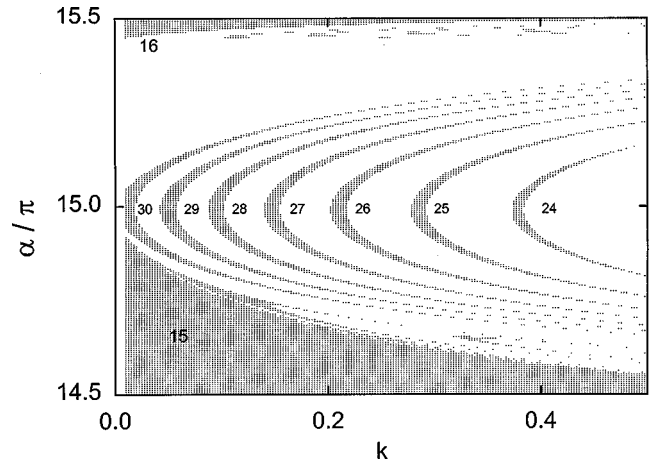


FIG. 4. Scan of the α - k plane. The region with black points shows the area where the short period chattering mode occurs. The numbers indicate the period of the mode in units of 2π . Here 2000 iterations were performed with initial conditions $t=0$ and $v=1$.

with Eq. (9) for which the maximum of the shock power is located very close to the saddle node bifurcation border. Thus, for L_M modes, the shock power does not increase with α only in the narrow region of their large noise sensitivity. It seems to be a rule that for resonant movement the shock power increases with α up to being replaced by a more noise-resistant mode, resulting in a strong reduction of shock power.

(v) Shock power in the nearly conservative region. When κ approaches zero, the system becomes nearly conservative. The behavior of such systems has been discussed in the literature [15]. In this region, persistent chaotic motion disappears and irregular movement is attracted by sinks which are stable orbits [15,7]. The shock power of L_M modes in that region follows from an expansion of Eq. (9) in the small parameter $\kappa/\pi M$:

$$p = \frac{2(1+\alpha)^2\kappa}{(\pi M)^3} \left[1 + O^2\left(\frac{\kappa}{\pi M}\right) \right]. \quad (10)$$

It seems to be a rule that, for any resonance, the shock power is proportional to κ in the nearly conservative region. This conclusion is based on a full analysis for L_M resonances and only on computer simulations for other modes studied. An example will be given in Sec. VI.

B. One quasiperiod of α

When α increases and k is not close to 1, resonances become sensitive to the noise and only chattering modes or long-period movements are observed. The areas where short-period chattering modes exist from characteristic regions which are nearly periodic in α with period π . An example corresponding to such a quasiperiod in α , $\pi(n-1/2) < \alpha < \pi(n+1/2)$, $n=15$, is shown in Fig. 4 and will be briefly discussed below.

The regions with the simplest chattering modes of $\{02\}$ type are displayed by cones: the large one corresponds to $T=2\pi n$ and is located over the horizontal line $\alpha=(n-1/2)\pi$, while the small one corresponding to $T=2\pi(n$

+1) is located below the horizontal line $\alpha=(n+1/2)\pi$; see Fig. 4.

Between the two cone-shaped areas discussed there exists a series of regions, each one having a characteristic crescent shape. The mode corresponding to the smallest value of k and $\alpha=\pi n$ has a period equal to $4\pi n$. The next crescent shapes located at a larger value of k correspond to periods $2\pi(n-1), 2\pi(n-2), 2\pi(n-3), \dots$, respectively. All the modes discussed correspond to the movement of $\{002\}$ type. In Fig. 1, an example of such a mode for $n=1$ is shown ($\alpha=2.20$). Below, we give an approximate location of the k_{nm} value corresponding to the center of the crescentlike shape for $\alpha=\pi n$, where $2\pi m$ is the period of the movement. The ball after chattering at time $t_i=0$ leaves the plate with velocity equal to 1, and interacts with the wall and plate at time $t_{i+1}=2\pi n$. After this shock the ball leaves the plate with velocity $v=2k_{nm}+1$, interacts with the wall, and arrives at the plate at time t_{i+2} :

$$2\pi m - \frac{3}{2}\pi < t_{i+2} - t_{i+1} < 2\pi m, \quad m=2n, 2n-1, 2n-2, \dots \quad (11)$$

Because

$$t_{i+2} - t_{i+1} = \frac{2\alpha}{2k_{nm} + 1}, \quad (12)$$

we have

$$\frac{2n-m}{2m-2n} < k_{nm} < \frac{8n-4m+3}{8m-8n-6}. \quad (13)$$

From inequality (13) and condition $0 \leq k \leq 1$, we get that the number of crescentlike shapes is approximately equal to $2n/3$.

Up to now we have considered only modes with one reflection from the wall between shocks. For every such mode we emphasize the existence of a new family of more complicated modes and the resulting picture in the α - k plane becomes very complex. So we will not go into more details.

VI. SHOCK POWER IN THE NONRESONANT REGION

Computer simulations with the NDIC show that the region of α between $(n-1/2)\pi$ and $(n+1/2)\pi$ can be divided into three parts: a region where short- and long-period chattering modes are present, extending from $k=0$ to moderate values of k , a region with transient chaotic movement, and a region for k very close to 1 (small dissipation). To illustrate it we perform a scan of the shock power for $\alpha=n\pi$, $n=15$; see Fig. 5. In the first part, dissipated power shows strong oscillations when the parameter k leaves one short-period shape and enters into another. When k increases, oscillations have a larger period, equal to $k_{nm+1}-k_{nm}$ according to Eq. (13). For k approaching 1, the system becomes nearly conservative: see Sec. V A. The straight line in Fig. 5 for $k>0.9$ does not correspond to a simple mode L_M , but in agreement with Eq. (10), the shock power is proportional to κ .

When the shock power is averaged over α between $\pi(n-1/2)$ and $\pi(n+1/2)$ in a nonresonant region, it exhibits a

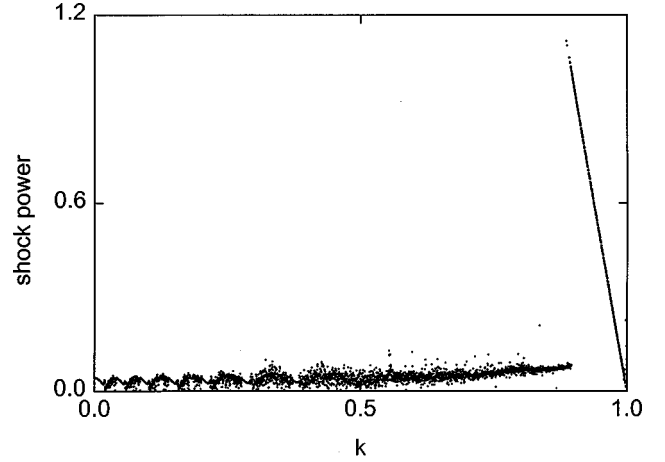


FIG. 5. Shock power versus k for $\alpha=15\pi$. The initial conditions were prepared by the NDIC: $I=0.05$, $b=0.01$, and 10 000 iterations were performed.

regular dependence; see Fig. 6. The data from Fig. 6 were fitted by a straight line, and the resulting expression for the shock power is given by

$$p = C\alpha^{-1}\kappa^\gamma, \quad (14)$$

where $C=0.91(1)$ and $\gamma=0.55(1)$

This shock power may be compared with a shock power of the L_M resonance. We see that when the resonance having a maximum shock power dissipated is destroyed and the system enters into irregular movement, the shock power decreases by a factor of f , where

$$f = \frac{2}{C} \left(\frac{\alpha}{\pi M} \right)^{2+\gamma}. \quad (15)$$

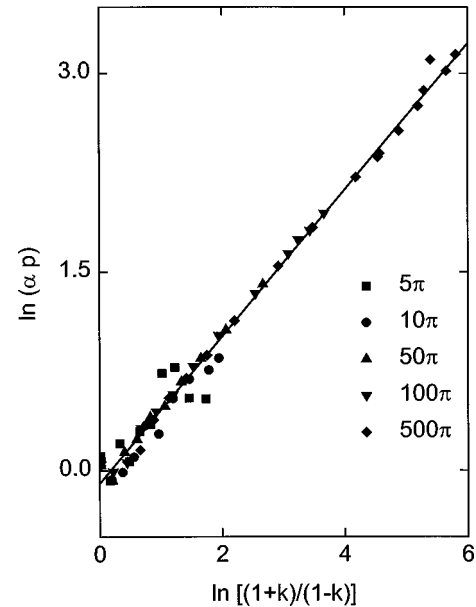


FIG. 6. Dependence of the shock power on the restitution coefficient. Each point corresponds to the averaging over α of 100 points lying between $\alpha-\pi/2$ and $\alpha+\pi/2$. The initial conditions were prepared by the NDIC: $I=0.02$, $b=0.01$, and 6000 iterations were performed and the first 1000 were omitted.

For κ close to zero and for the L_M mode, the f factor is equal to

$$f = \frac{2\alpha(1+\alpha)^2\kappa^{\gamma-1}}{(\pi M)^3 C} \left[1 + O^2\left(\frac{\kappa}{\pi M}\right) \right]. \quad (16)$$

Equation (16) follows from Eqs. (10) and (14).

VII. EXPERIMENTAL DETAILS

The experimental setup consists of an air track and a horizontally moving object with a mass of 61.15 g. The air flow of the air track allowed nearly free horizontal movement of the object. On one end of the object a steel spring is attached which interacts with a rigid steel wall. The other end of the object has a rounded shape made of steel of the approximate radius of 1 mm. This end interacts with the moving plate covering by tin alloy. The microhardness of the alloy measured at different points ranges from $7H_v$ to $11H_v$. The distance between the mean position of the vibrating plate and the wall was measured by a micrometer screw with a resolution of $1\mu\text{m}$.

The Mössbauer transducer of MA250 FAST Comtec type was used as a vibrating plate, serving high-quality movement. An additional 357 g of mass was attached to the transducer, which reduces influence of the shock on the movement of the transducer. The transducer was moving in a sinusoidal mode with a frequency of $5.152(2)$ Hz. The velocity amplitude measured by the laser interferometer was equal to $1.218(1)$ mm/s. The so-called error signal, which is the difference between input signal of the transducer and reading of the pickup coil, was recorded. The error signal allows the determination of two relevant quantities: time of shock and its intensity.

A black fingerprint drawing on transparent sheet was attached to the body, allowing optical measurement of the velocity of the moving object. The precision of the velocity measurement was better than 2%.

Three signals were recorded simultaneously with a sampling frequency 5 kHz: the error signal, the velocity of the object, and the input signal of the transducer, which is proportional to the velocity of the plate. From these signals the shock phase and velocity before and after shock were determined. The measured values of the coefficient of restitution were $0.83(3)$ for the wall-spring and $0.54(8)$ for the plate-tin alloys.

The measured velocities and phases of the shocks allow in principle the determination of the dissipated shock power. However, two experimental problems arise: (i) when shocks occur close to each other, it is difficult to measure the velocity, and (ii) when shock energy is small, it remains difficult to separate shock signal from the noise; see the example in Fig. 7. To overcome these difficulties, we apply a measurement procedure of shock intensity which does not depend on the details of the recorded signal, and then we use calibration for estimating absolute shock power. Details of the procedure are given below.

The measured quantity ε_a , directly dependent on the energy dissipated during the recording time $t_N - t_1$, is defined arbitrarily as

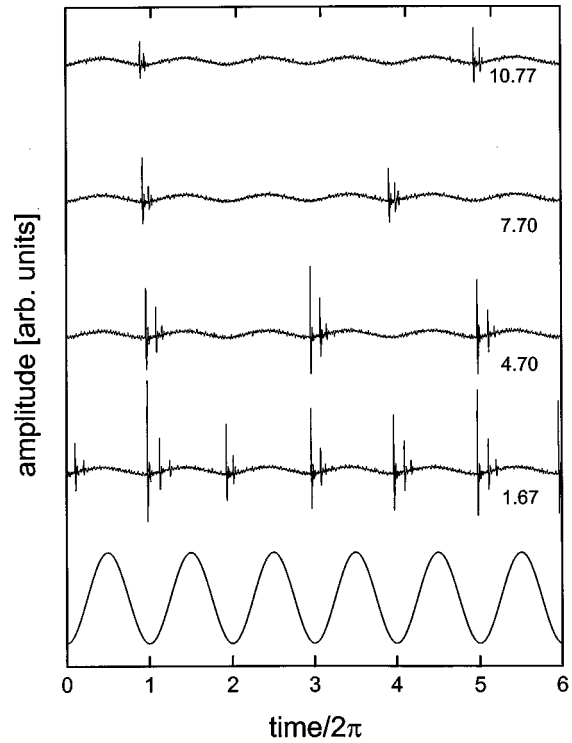


FIG. 7. Error signal for the sequence of simplest chattering modes of $\{02\}$ type. In the model, these modes are located at $\alpha = (2n-1)/2\pi$, $n=1,2,3,4$. Below, the sinusoid indicates the position of the plate.

$$\varepsilon_a = \sum_{i=1}^N (|s_i| - b), \quad (17)$$

where s_i is the error signal after removing sinusoidal background component and b is the mean value of the $|s_i|$ in the regions where shocks are not present. Then, for a few periodic modes with well-separated shocks (see the examples in Fig. 8 for $\alpha = 14.10, 7.53$, and 3.76), ε_a have been measured for each shock. Independently, velocities of the object before, v_b , and after shock, v_a , were measured by optical method. The velocity of the plate, v , was determined from the recorded time of the shock. Next, the dissipated energy of each shock was estimated:

$$\varepsilon = (v_b - v)^2 - (v_a - v)^2. \quad (18)$$

Its dependence on ε_a is plotted in Fig. 9, together with the calibration curve. Both curves Eqs. (3c) and (17), were together used for the determination of the shock power of any type of movement.

Our apparatus was only an approximation of the one-dimensional, two-parameter model considered. The main sources of disagreement are listed below.

(i) As previously mentioned, the interaction with the wall was not elastic in our experimental setup. It is possible to renormalize variables and to introduce an effective restitution coefficient which takes this effect into account for modes of L_M type, but it is not possible for general movement.

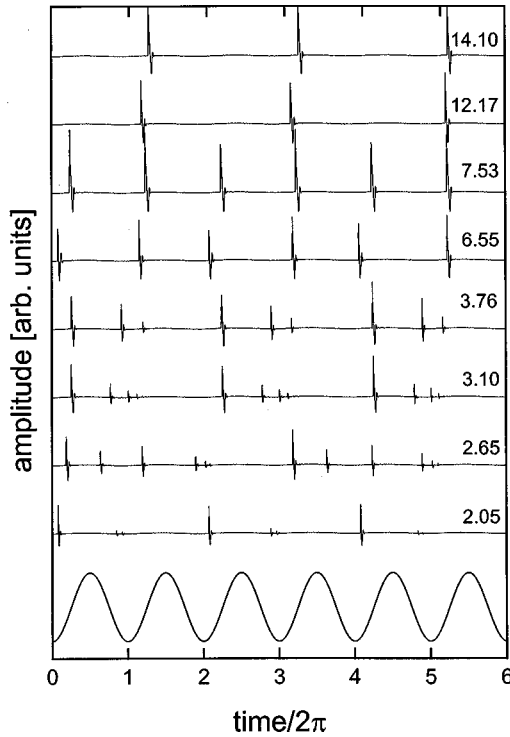


FIG. 8. Error signal for sequence of periodic modes for different values of α (indicated by numbers). Below, the sinusoid indicates the position of the plate.

(ii) In the case of small velocities, the movement was disturbed by the inhomogeneous airflow of the used airtrack. So it was not possible to perform experiments with nonresonant movement at large α .

(iii) The shocks induce on the moving body small perpendicular vibrations which disturb the longitudinal movement. In some cases we were able to record only short series of the resonant movement.

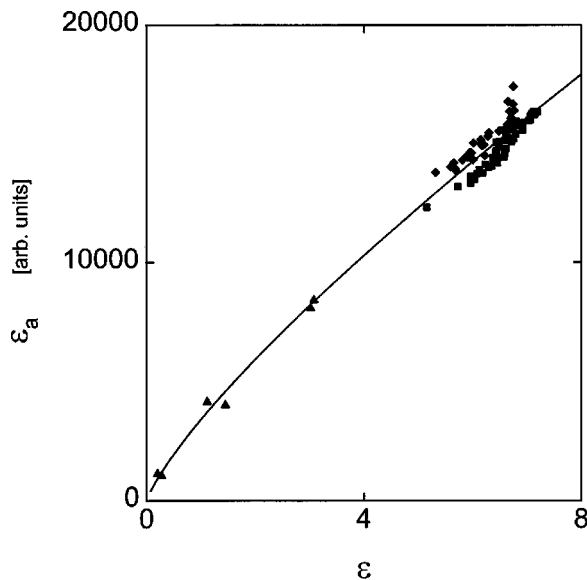


FIG. 9. Calibration curve for the shock energy; see the text. Directly measured dissipated energy is shown on the horizontal axis. Squares and diamonds correspond to L_M , $M=1,2$, modes, respectively, while triangles to the mode of $\{001\}$ type shown in Fig. 1 for $\alpha=3.94$.

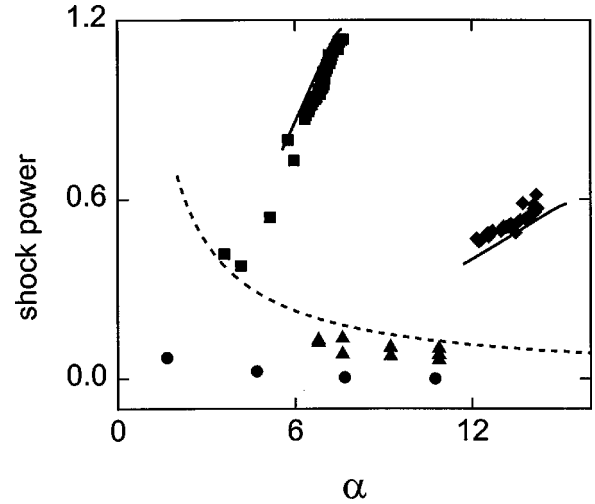


FIG. 10. Measured shock power versus α . Squares and diamonds correspond to L_M , $M=1,2$, modes, respectively, triangles to the nonresonant mode, and circles to the silent modes. The solid lines correspond to the resonant movement for the restitution coefficients of the wall and of the plate equal to 0.815 and 0.53, respectively. The dashed line corresponds to Eq. (14) for $k=0.35$.

We detected experimentally the gain of the shock power when the system enters into the resonant mode. The results are shown in Fig. 10. The solid lines represent the shock power for L_M modes for the model in which the restitution coefficient of the wall is different than 1 (partially elastic collisions with the wall).

The evolution of the periodic modes when α is varied is presented in Fig. 8. Doubling of the period was detected for the L_2 mode (see $\alpha=14.10$ and 12.17 in Fig. 8) as well as for the L_1 mode (see $\alpha=7.53$ and 6.55 in Fig. 8). The four last examples from Fig. 8 correspond to the sequence of exact solutions shown in Fig. 1. Figure 7 shows the sequence of the simplest chattering (silent) modes. The values of α found experimentally (see the numbers in Fig. 7) are close to those predicted in our model: they occur in the region of cones located at $\alpha=\pi/2$, $3\pi/2$, $5\pi/2$, and $7\pi/2$. The measured shock power of the silent modes, which is much smaller than the others, is shown in Fig. 9. All the modes detected experimentally have their analogs in the model studied numerically.

VIII. CONCLUSIONS

The α - k plane may be divided into two characteristic regions: a part in which strong resonances are present and a part with nonresonant movement. Computer simulations with the NDIC serve as a tool for finding the most noise resistant modes.

The resonances which are more noise resistant than nonresonant modes occur in the region with a small restitution coefficient where the system is nearly conservative and in the region where α/π has an order of magnitude equal to 1. For the regions of the α - k plane with resonances resistant against external noise, the behavior of the shock power seems to follow the following rules: (i) in the nearly conservative region, the shock power is proportional to $(1-k)/(1+k)$, (ii) for a given resonance, the shock power increases

with α , (iii) the decrease of α leads to a period-doubling route to chaos which does not change the character of the dependence of the shock power on α , (iv) the transition from the resonant to nonresonant region is associated with a reduction of the dissipated power. Behavior consistent with the above statements has been observed in computer simulations while (ii), (iii), and (iv) only in the present experiments.

In the nonresonant region, two main types of movement are present: short period chattering and long period or chaotic. Chattering modes for a given short period occur in the regions of the α - k plane forming quasiperiodic patterns. The shock power after averaging over one quasiperiod of α is described by the equation covering the whole nonresonant region. In contrast with the resonant region, the shock power in the nonresonant region is inversely proportional to α and increases with k .

An open question is the behavior of the model with more than one moving object. Indeed, it was reported that such macroscopic systems with dissipation can reach strange states which violate equipartition of energy [16]. It thus would be interesting to extend the estimation of the energy dissipation in many-particle models.

ACKNOWLEDGMENTS

One of authors K.S. acknowledges the hospitality of the LPEC and a grant for the Region Pays de la Loire. The authors thank B. Gazengel and E. Mariez (IAM Le Mans) for a calibration of the measurements of the transducer, and Dr. J. M. Greneche for a critical reading of the manuscript.

-
- [1] E. Fermi, *Phys. Rev.* **75**, 1169 (1949).
 - [2] S. Ulam, in *Proceedings of the 4th Berkeley Symposium on Mathematical Statistics and Probability* (University of California Press, Berkeley, 1961), Vol. 3, p. 315.
 - [3] M. A. Lieberman and A. J. Lichtenberg, *Phys. Rev. A* **5**, 1852 (1972).
 - [4] A. J. Lichtenberg, M. A. Lieberman, and R. H. Cohen, *Physica D* **1**, 291 (1980).
 - [5] A. Mehta and J. M. Luck, *Phys. Rev. Lett.* **65**, 393 (1990).
 - [6] J. M. Luck and A. Mehta, *Phys. Rev. E* **48**, 3988 (1993).
 - [7] Z. J. Kowalik, M. Franaszek, and P. Pieranski, *Phys. Rev. A* **37**, 4016 (1988).
 - [8] B. Drosel and T. Prellberg, *Eur. Phys. J. B* **1**, 533 (1998).
 - [9] A. Valance and D. Bideau, *Phys. Rev. E* **57**, 1886 (1998).
 - [10] D. Maurice and T. H. Courtney, *Metall. Mater. Trans. A* **26**, 2431 (1995).
 - [11] M. Abdellaoui and E. Gaffet, *Mater. Sci. Forum* **179-181**, 339 (1995).
 - [12] M. P. Dallimore and P. G. McCormick, *Mater. Sci. Forum* **235-238**, 5 (1997).
 - [13] S. W. Shaw and P. J. Holmes, *J. Sound Vib.* **90**, 129 (1983).
 - [14] A. H. Nayfeh and B. Balachandran, *Applied Nonlinear Dynamics* (Wiley, New York, 1995).
 - [15] M. A. Lieberman and K. Y. Tsang, *Phys. Rev. Lett.* **55**, 908 (1985). K. Y. Tsang and M. A. Lieberman, *Physica D* **21**, 401 (1986).
 - [16] Y. Du, H. Li, and L. P. Kadanoff, *Phys. Rev. Lett.* **74**, 1268 (1995).